This article has been accepted for publication in a future issue of this journal, but has not been fully edited. Content may change prior to final publication. Citation information: DOI 10.1109/TSG.2016.2572639, IEEE Transactions on Smart Grid

Energy and Reserve Scheduling under Wind Power Uncertainty: An Adjustable Interval Approach

Meysam Doostizadeh, Farrokh Aminifar, *Senior Member, IEEE*, Hassan Ghasemi, *Senior Member, IEEE*, and Hamid Lesani

***Abstract*—This paper presents an adjustable interval optimization (AIO) model for the energy and reserve clearance while treating the wind power variation and uncertainty. Instead of conventional predicted intervals (PIs), adjustable intervals (AIs) as subsets of PIs are proposed as more judicious choices for economically covering wind uncertainties. Ramp-capability reserve is modeled to ensure the existence of sufficient ramp capability needed to follow up wind power variation within AIs. However, realization of wind power beyond AIs, which is no longer compensable by ramp-capability reserve, would necessarily lead to either load shedding or wind spillage. In order to optimally determine AIs, apart from the energy and reserve procurement costs, the costs associated with load shedding and wind spillage are incorporated in the objective function. The confidence level theory is employed as well for tuning the robustness and conservatism of the final solution. Performance of the proposed method is examined on several case studies on an 8-bus and modified IEEE 118-bus test systems. Sensitivity analyses are conducted to specify the impacts of important parameters on the obtained solution. The results confirm the applicability and effectiveness of the proposed methodology.**

***Index Terms*—Day-ahead market energy and reserve scheduling, ramping capability, wind power uncertainty.**

NOMENCLATURE

A. Sets and Indices

i	Index of conventional generating units (1 to N_G).
j	Index of wind farms (1 to N_J).
b	Index of buses and loads (1 to N_B).
t	Index of time periods (1 to N_T).
s	Index of probability intervals (1 to N_S).
l	Index of transmission lines.
Γ	Set of lines.
J_b	Set of wind farms connected to bus b.
I_b	Set of conventional generating units connected to bus b.

B. Parameters

T_i^{DN} / T_i^{UP}	Minimum down/up time [h].
T_i^{ON} / T_i^{OFF}	The number of initial periods during which the unit must be online/off-line.
SD_i / SU_i	Shut-down/Start-up ramp limit [*MW/h*].
RD_i / RU_i	Ramp-down/up limit [*MW/h*].
C_{it}^{SU} / C_{it}^{SD}	Start-up/shut-down cost [*$*].
q_{it}^{dn} / q_{it}^{up}	Price offer for downward/upward power-capacity reserve [*$/MWh*].
C_{it}^{F}	Fixed running cost [*$/h*].
C_{it}^{V}	Variable generation cost [*$/MWh*].
$\overline{r_i^{up}}$ / $\overline{r_i^{dn}}$	Maximum of r_{it}^{up} / r_{it}^{dn} [*MW*].
C_t^{EENS}	Cost of energy not supplied [*$/MWh*].
C_t^{EWS}	Cost of wind energy spillage [*$/MWh*].
$\overline{P_i^G}$ / $\underline{P_i^G}$	Maximum/minimum of P_{it}^G [*MW*].
P_{jt}^W	Wind power forecast as offered in the market [*MW*].
$\tilde{P}_{jt}^W$	Possible wind farm power output of [*MW*].
$\overline{P_{jt}^W}$, $\underline{P_{jt}^W}$	Predicted interval (PI) of P_{jt}^W.
$\overline{F_l}$	Maximum capacity of line l [MW].
K_{li}	Generation distribution shift factor.
$fr(l)$ / $\text{to}(l)$	Sending/receiving bus of line l.
D_{bt}	Demand power [*MW*].
α	Predefined confidence level.
$\bar{\Phi}^{\alpha}$ / $\underline{\Phi}^{\alpha}$	α-dependent confidence boundaries.
σ_t	Standard deviation of total wind power forecast error.
$\pi_{t,s}$	Discretized probability distribution function.

C. Variables

u_{it} / w_{it}	Binary variable indicating start-up/shut-down.
v_{it}	Binary variable indicating unit commitment status.
$\overline{\hat{P}_{jt}^W}$, $\underline{\hat{P}_{jt}^W}$	Adjustable interval (AI) of P_{jt}^W [*MW*].
P_{it}^G	Scheduled Power [*MW*].
$\tilde{P}_{it}^G$	Possible output power of generating unit [*MW*].
$\hat{P}_{it}^G$	Generating unit output power under the network worst-case scenario [*MW*].
r_{it}^{up} / r_{it}^{dn}	Downward/upward power-capacity reserve [*MW*].
$EENS_t$	Expected energy not supplied [*MWh*].
EWS_t	Expected wind energy spillage [*MWh*]
$L_{t,s}^{shed}$	Load shedding amount [*MW*].

M. Doostizadeh, F. Aminifar, and H. Lesani are and H. Ghasemi was with the School of Electrical and Computer Engineering, College of Engineering, University of Tehran, North Kargar Ave., Tehran, 11365-4563, Iran. (e-mail: m.doostizadeh@ut.ac.ir, faminifar@ut.ac.ir, hassan.ghasemi@ieee.org, lesani @ut.ac.ir).

This article has been accepted for publication in a future issue of this journal, but has not been fully edited. Content may change prior to final publication. Citation information: DOI 10.1109/TSG.2016.2572639, IEEE Transactions on Smart Grid

$P_{t,s}^{spill}$ Wind power spillage [*MW*].

I. Introduction

FLEXIBILTY is the ability of a power system within an acceptable lead time to anticipate and adapt to the system net load, load minus variable generation, changes [1]. High penetration of renewable energy sources, especially wind power plants, has the potential to affect the flexibility of the system due to their inherent intermittency and imperfect predictability. Variation and uncertainty of wind generation could be absorbed by effectively scheduling and deployment of reserves. Additionally, anticipation can be interpreted as the prediction of these variations and uncertainties.

A conservative solution to deal with this uncertainty is to increase the reserve across the power system. However, such a solution certainly imposes higher operation costs. In order to devise an effective and robust methodology to deal with wind uncertainties, many research works have so far been conducted. A few independent system operators (ISOs) across the US such as, California ISO [2] and Midcontinent ISO [3], have applied flexible ramping product in their real practices. The main characteristic of this method is providing ramping ability to deal with the expected maximum variation of wind power generation in both upward and downward directions. Having applied this technique, ISOs are able to enhance the robustness of load following reserve, which in turn promotes the effectiveness of operation. This technique does not explicitly consider the stochastic nature of problem.

Stochastic optimization (SO) has been recommended as a solution to deal with wind power uncertainty in the unit commitment problem [4]-[6]. SO employs several scenarios along with their associated probabilities for simulating possible realizations of uncertainties. The accuracy and optimality of the SO solution strongly depend on the accuracy of probability distribution of uncertain variables as well as the number of scenarios considered within the optimization problem. A large set of scenarios, although can improve the accuracy of solution, renders the problem computationally intractable [7]. In such cases, scenario reduction techniques can reduce the size of SO model and consecutively lessen the computational effort [8], [9]. However, even with a scenario reduction technique, the monetary benefits as well as the system security may not perfectly be attained [10], [7].

Chance-constrained optimization (CCO) is another method in which system security constraints can be violated with a small predefined level of probability [11]-[13]. In case of having non-Gaussian probability distribution of uncertain parameters, CCO is usually non-convex and might be intractable in large-scale power systems [14].

To improve the system security, robust optimization (RO) allows wind generation fluctuations within a given range around a central forecast [14]-[17]. Since RO is based on uncertainty sets and minimizes cost of the worst-case scenario, this method results in an overly conservative solution as compared to SO [18]. The budget of uncertainty [19] or dynamic uncertainty sets [20] are presented to adjust the conservatism of RO; however, there exists no systematic methodology to choose the level of conservatism.

In the interval optimization (IO), the operating cost of the central forecast is minimized while enforcing the feasibility of transitions within given ranges, commonly referred to as predicted intervals (PIs), around the central forecast [10], [21], [22]. Compared to SO, the IO yields more conservative schedules and demands less computational efforts [10]. Compared to RO, IO generates less precise results since RO is based on the worst-case scenarios of uncertainty.

In order to improve the solution quality and/or enhance the computational performance, hybrid approaches have also been presented. In [23], SO was applied on initial operating hours during which wind power forecasts are more accurate. Then, it was switched to the interval formulation for the remaining hours, in order to balance the operating cost and the solution robustness. In [18], a hybrid SO and RO was presented to provide a more robust and computationally tractable method as compared to SO, and a more cost-effective decision as compared to RO. Also, references [24] and [25] proposed algorithms to discard a vast majority of the security constraints in the high-dimensional security constrained unit commitment and security constrained optimal power flow problems, respectively, in order to arrive at an equivalent reduced-order problem which can be solved significantly faster.

In view of the above concerns, each of the methods reported in the literature has its own advantages in modeling the uncertainty; however, the optimality and robustness of the solution and their compromise are still a matter of concern when applied to practical market clearing. In the search of an algorithm that is adjustably robust and computationally efficient at the same time, this paper proposes an adjustable interval optimization (AIO) model for day-ahead energy and reserve market clearing while treating the variation and uncertainty of wind generation. The major purpose of new method is to improve the security of power system with high wind power penetration against associated variability and uncertainty. The main contributions of the proposed AIO model can be summarized as follows:

1) The proposed market clearing model incorporates adjustable intervals (AIs) instead of conventional PIs to deal with wind generation uncertainty in an economic way. The model seeks optimal commitment decisions that ensure that sufficient reserves are available to adapt to any realization of wind power uncertainties within the calculated AIs. The costs imposed by uncertainties not compensated by the ramping capability reserve are considered as penalties and minimized in the objective function. At the same time, a chance constraint is proposed to make the level of conservatism adjustable.
2) Apart from the day-ahead power-capacity reserve, ramp-capability reserve is also considered to guarantee that the committed generating units will be able to cope with the expected maximum ramp of wind power variation within AIs. To do so, the proposed formulation models the interdependency between ramp-capability reserve and power-capacity reserve provided by each generating unit.
3) The proposed mixed integer linear programming (MILP) model only needs two upward and downward reserve constraints; hence, it is very computationally efficient and applicable in real-scale systems.

This article has been accepted for publication in a future issue of this journal, but has not been fully edited. Content may change prior to final publication. Citation information: DOI 10.1109/TSG.2016.2572639, IEEE Transactions on Smart Grid

II. Proposed Methodology

For the sake of clarification, the interval optimization model for day-ahead market clearing under wind power uncertainty is first formulated in Section II.A where the level of conservatism is not adjustable. Next, the proposed AIO model is given in Section II.B.

A. Interval Optimization Model under Wind Power Uncertainty

It is supposed that conventional generating units submit their economic data along with technical limitation. Also, wind power producers offer their forecasted production (P_{jt}^{W}) along with PIs [$\underline{P_{jt}^{W}}, \overline{P_{jt}^{W}}$] for the following day. The upper and lower bounds of PIs are respectively denoting the maximum and minimum deviations that each wind farm may encounter. Ultimately, the ISO clears the market according to the system load forecasts at every hour for 24-h time horizon and find out the optimal energy and reserve dispatch. Note that the reserve is generally scheduled for handling possible contingencies, load changing and uncertainty, and wind power variation and uncertainty. However, as the main focus of this paper, only wind power uncertainty is considered while the others can be also accounted for by slight modifications. The problem in question is formulated as an optimization model (1)-(14). The objective function (1) consists of start-up costs, shut-down costs, and energy and reserve costs over the scheduling horizon, respectively. The operating costs of wind farms are assumed to be zero while any other assumption can be easily added. The problem constraints include power balance constraint (2), line flow capacity limits (3), unit minimum ON and OFF time limits (4), logical commitment constraints (5), unit generation plus reserve limits (6) and (7), unit ramping up and down limits (8) and (9), and unit upward and downward scheduled reserves limits (10) and (11). Constraints (12) - (14) guarantee that any realization of wind power uncertainty is tolerable by redispatch of generating units. Similar to (2) and (3), expressions (12) and (13) are the power balance and the network constraints, respectively, when the wind uncertainty is revealed. It is worth mentioning that load uncertainty can be added on the right hand of constraint (12) as well. Constraint (14) states that the difference between the redispatch of the generating units and their scheduled power is limited to the amount of upward/downward reserve quantities awarded in the market.

$$\min \sum_{t=1}^{N_T}\sum_{i=1}^{N_G}(u_{it}C_{it}^{SU}+w_{it}C_{it}^{SD}+v_{it}C_{it}^{F}+C_{it}^{V}P_{it}^{G}+q_{it}^{up}r_{it}^{up}+q_{it}^{dn}r_{it}^{dn}) \quad (1)$$

$$\sum_{i=1}^{N_G}P_{it}^{G}+\sum_{j=1}^{N_J}P_{jt}^{W}=\sum_{b=1}^{N_B}D_{bt} \quad (2)$$

$$-\overline{F_l}\le\sum_{b=1}^{N_B}K_{lb}\left(\sum_{i\in I_b}P_{it}^{G}+\sum_{j\in J_b}P_{jt}^{W}-D_{bt}\right)\le\overline{F_l},\ \forall l\in\Gamma \quad (3)$$

$$\begin{cases} v_{it}=v_{i,t_0} & \forall t\in\left[0,T_i^{ON}+T_i^{OFF}\right] \\ \sum_{h=t-T_i^{UP}+1}^{t}u_{ih}\le v_{it} & \forall t\in\left[T_i^{ON},N_T\right] \\ \sum_{h=t-T_i^{DN}+1}^{t}w_{ih}\le 1-v_{it} & \forall t\in\left[T_i^{OFF},N_T\right] \end{cases} \quad (4)$$

$$\begin{cases} u_{it}-w_{it}=v_{it}-v_{i,t-1} \\ u_{it}+w_{it}\le 1 \end{cases} \quad (5)$$

$$P_{it}^{G}+r_{it}^{up}\le v_{it}\overline{P_i^{G}} \quad (6)$$

$$P_{it}^{G}-r_{it}^{dn}\ge v_{it}\underline{P_i^{G}} \quad (7)$$

$$\begin{cases} P_{it}^{G}-P_{i,t-1}^{G}\le RU_i v_{i,t-1}+SU_i(v_{it}-v_{i,t-1})+\hat{M}(1-v_{it}) \\ \hat{M}=\max(0,SU_i-RU_i-\underline{P_i^{G}}) \end{cases} \quad (8)$$

$$\begin{cases} P_{i,t-1}^{G}-P_{it}^{G}\le RD_i v_{it}+SD_i(v_{i,t-1}-v_{it})+\hat{N}(1-v_{i,t-1}) \\ \hat{N}=\max(0,SD_i-RD_i-\underline{P_i^{G}}) \end{cases} \quad (9)$$

$$0\le r_{it}^{up}\le v_{it}\overline{r_i^{up}} \quad (10)$$

$$0\le r_{it}^{dn}\le v_{it}\overline{r_i^{dn}} \quad (11)$$

$$\sum_{i=1}^{N_G}\tilde{P}_{it}^{G}+\sum_{j=1}^{N_J}\tilde{P}_{jt}^{W}=\sum_{b=1}^{N_B}D_{bt},\quad \forall\tilde{P}_{jt}^{W}\in\left[\underline{P_{jt}^{W}},\overline{P_{jt}^{W}}\right] \quad (12)$$

$$-\overline{F_l}\le\sum_{b=1}^{N_B}K_{lb}\left(\sum_{i\in I_b}\tilde{P}_{it}^{G}+\sum_{j\in J_b}\tilde{P}_{jt}^{W}-D_{bt}\right)\le\overline{F_l},\ \forall l\in\Gamma \quad (13)$$

$$-r_{it}^{dn}\le\tilde{P}_{it}^{G}-P_{it}^{G}\le r_{it}^{up} \quad (14)$$

For all possible uncertain parameters ($\tilde{P}_{jt}^{W}$) within the PIs, (12) and (13) can be inferred as the system security assurance. If the worst-case scenarios are tolerable, any other realization of uncertain parameters would not be problematic. As proved in the Appendix, four worst-case scenarios associated with the wind power lower and upper limit productions are to be incorporated. The lower limit of the wind power generation imposes a constraint on the upward reserve, (15).

$$\sum_{i=1}^{N_G}P_{it}^{G}+\sum_{i=1}^{N_G}r_{it}^{up}+\sum_{j=1}^{N_J}\underline{P_{jt}^{W}}=\sum_{b=1}^{N_B}D_{bt} \quad (15)$$

The downward reserve constraint corresponds to the upper limit of wind power generation, that is

$$\sum_{i=1}^{N_G}P_{it}^{G}-\sum_{i=1}^{N_G}r_{it}^{dn}+\sum_{j=1}^{N_J}\overline{P_{jt}^{W}}=\sum_{b=1}^{N_B}D_{bt} \quad (16)$$

Also, transmission limits under the worst-case scenario associated with the wind power lower and upper limit productions should be ensured by

$$\begin{cases} -\sum_{j=1}^{N_J}\xi_{ljt}+\sum_{i=1}^{N_G}K_{li}\hat{P}_{it}^{G}+\sum_{j=1}^{N_J}K_{lj}\overline{P_{jt}^{W}}-\sum_{b=1}^{N_B}K_{lb}D_{bt}\le\overline{F_l} \\ \xi_{ljt}\ge 0,\ -\xi_{ljt}\le K_{lj}\left(\underline{P_{jt}^{W}}-\overline{P_{jt}^{W}}\right) \end{cases} \forall l\in\Gamma \quad (17)$$

$$\begin{cases} \sum_{j=1}^{N_J}\vartheta_{ljt}+\sum_{i=1}^{N_G}K_{li}\hat{P}_{it}^{G}+\sum_{j=1}^{N_J}K_{lj}\overline{P_{jt}^{W}}-\sum_{b=1}^{N_B}K_{lb}D_{bt}\ge-\overline{F_l} \\ \vartheta_{ljt}\ge 0,\ \vartheta_{ljt}\ge K_{lj}\left(\underline{P_{jt}^{W}}-\overline{P_{jt}^{W}}\right) \end{cases} \forall l\in\Gamma \quad (18)$$

This article has been accepted for publication in a future issue of this journal, but has not been fully edited. Content may change prior to final publication. Citation information: DOI 10.1109/TSG.2016.2572639, IEEE Transactions on Smart Grid

where ξ_{ljt} and ϑ_{ljt} are the dual variables of constraints in (A10) and (A11), respectively; $\hat{P}_{it}^{G}$ is the output power of generating unit *i* under the network worst-case scenario and takes the place of $\tilde{P}_{it}^{G}$ in (14).

B. Adjustable Interval Optimization (AIO) Model

The major concern associated with the interval optimization model is that by the rise of wind power prediction error, the model may turn to be extremely conservative. To alleviate this drawback, the proposed AIO model incorporates AIs instead of conventional PIs to deal with wind generation uncertainty in an economic way. To do so, the following modifications are proposed.

1) Objective function: The new objective function (19) contains two sums: the former is the operation cost of conventional units as presented in Section II.A. The latter sum represents the costs related to wind power uncertainties not covered by the reserve capacities. These low probable events cause either load shedding or wind spillage depending on the wind power shortage or surplus, respectively. The expected energy associated with load shedding and wind curtailment are respectively denoted by expected energy not supplied (EENS) and expected wind energy spillage (EWS). The costs associated with these events are added to the objective function as the penalty factors letting ISO optimally determine the reserve values. Fig. 1 depicts the total wind power uncertainty and probable load shedding and wind spillage situations. The larger interval covered by the system ramping reserve, the lower load shedding and wind spillage is expected. The probability distribution of wind power forecast error from individual wind turbine is not Gaussian. A large number and geographically dispersed wind turbines, however, allow the implementation of central limit theory [26] to supports the assumption of Gaussian distribution of the total wind power forecast error. Here, Gaussian distribution is used for the sake of demonstration and any other probability distribution can be freely envisaged. Also, no probability distribution is deemed for individual wind turbines and having their power generation within the PIs is the only assumption.

$$z = \sum_{t=1}^{N_T}\sum_{i=1}^{N_G}(u_{it}C_{it}^{SU} + w_{it}C_{it}^{SD} + v_{it}C_{it}^{F} + C_{it}^{V}P_{it}^{G} + q_{it}^{up}r_{it}^{up} + q_{it}^{dn}r_{it}^{dn}) + \sum_{t=1}^{N_T}(C_t^{EENS}EENS_t + C_t^{EWS}EWS_t) \quad (19)$$

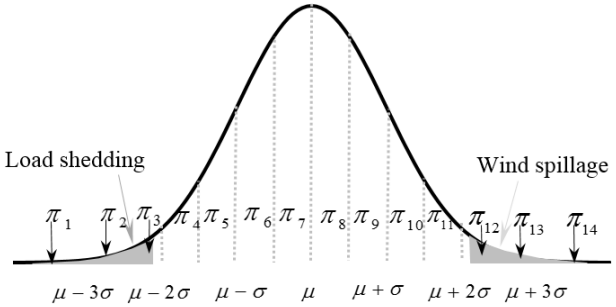

Fig. 1. 14-interval approximation of the Gaussian distribution.

2) Wind farms generation output constraints: Since AIO model optimally determines AIs of wind power output $[\underline{\hat{P}_{jt}^{W}}, \overline{\hat{P}_{jt}^{W}}]$ for each wind farm, upper and lower limits of AIs are the wind-dispatch variables that are constrained by their associated production forecast and PIs as presented in (20).

$$\underline{P_{jt}^{W}} \le \underline{\hat{P}_{jt}^{W}} \le P_{jt}^{W} \le \overline{\hat{P}_{jt}^{W}} \le \overline{P_{jt}^{W}} \quad (20)$$

In addition to the potential uncertainty cost added to the objective function, a chance constraint is also proposed to enable the operators to assure the conservativeness of the solutions according to their desired levels of system security. This constraint does not allow that the system security is overly threatened by the optimality aspect of system operation, (19). It is a probabilistic risk measure that guarantees the feasibility of solution within a predefined confidence level, i.e.

$$Pr(\underline{\Phi^{\alpha}} \le \sum_{j=1}^{N_J}\tilde{P}_{jt}^{W} \le \overline{\Phi^{\alpha}}) \ge 1-\alpha \quad (21)$$

Note that the lower and upper confidence boundaries ensure the variation of uncertain parameters $\tilde{P}_{jt}^{W}$ with the predefined confidence level $(1-\alpha)$. Knowing the confidence level of the chance constraint and the probability distribution function of the uncertain parameters, expression (21) can recast as

$$Pr(\sum_{j=1}^{N_J}P_{jt}^{W} - \gamma\sigma_t \le \sum_{j=1}^{N_J}\tilde{P}_{jt}^{W} \le \sum_{j=1}^{N_J}P_{jt}^{W} + \gamma\sigma_t) \ge 1-\alpha_{\gamma} \quad (22)$$

The left-hand side of this equation is the probability of having enough scheduled power-capacity reserve to address wind uncertainty $(\pm\gamma\sigma_t)$ and $(1-\alpha_{\gamma})$ is the associated confidence level. Considering lower and upper limits of the uncertain parameters $\tilde{P}_{jt}^{W}$ which are equal to lower and upper bounds of AIs, the chance-constrained can be converted to a deterministic equivalent as follows:

$$\sum_{j=1}^{N_J}\underline{\hat{P}_{jt}^{W}} \le \sum_{j=1}^{N_J}P_{jt}^{W} - \gamma\sigma_t \quad (23)$$

$$\sum_{j=1}^{N_J}P_{jt}^{W} + \gamma\sigma_t \le \sum_{j=1}^{N_J}\overline{\hat{P}_{jt}^{W}} \quad (24)$$

Although constraints (23) and (24) ensure sufficient scheduled power-capacity reserve to meet wind uncertainty with the desired confidence level, some actual wind power generation output might occur when $\overline{\hat{P}_{jt}^{W}} \le \tilde{P}_{jt}^{W}$ and $\tilde{P}_{jt}^{W} \le \underline{\hat{P}_{jt}^{W}}$ (Fig. 1). These situations would respectively lead to wind spillage, $\sum_{j=1}^{N_J}(\overline{P_{jt}^{W}} - \overline{\hat{P}_{jt}^{W}})$, and load shedding, $\sum_{j=1}^{N_J}(\underline{\hat{P}_{jt}^{W}} - \underline{P_{jt}^{W}})$. In order to calculate the probability of load shedding and wind spillage, the probability distribution of total wind power forecasted error is divided into even N_S intervals with the probability of $\pi_{t,s}$ and width of σ_t / n for each interval. Here, 14-interval approximation (n=2) is selected as illustrated in Fig. 1. Accordingly, $EENS_t$ and EWS_t are

$$EENS_t = \sum_{s=1}^{\frac{N_S}{2}}\pi_{t,s}L_{t,s}^{shed} \quad (25)$$

This article has been accepted for publication in a future issue of this journal, but has not been fully edited. Content may change prior to final publication. Citation information: DOI 10.1109/TSG.2016.2572639, IEEE Transactions on Smart Grid

$$\sum_{s=1}^{\frac{N_S}{2}} L_{t,s}^{shed} \geq \sum_{j=1}^{N_J} (\underline{\hat{P}_{jt}^W} - \underline{P_{jt}^W}) \tag{26}$$

$$0 \leq L_{t,s}^{shed} \leq \sigma_t / n \tag{27}$$

$$EWS_t = \sum_{s=\frac{N_S}{2}+1}^{N_S} \pi_{t,s} P_{t,s}^{spill} \tag{28}$$

$$\sum_{s=\frac{N_S}{2}+1}^{N_S} P_{t,s}^{spill} \geq \sum_{j=1}^{N_J} (\overline{P_{jt}^W} - \overline{\hat{P}_{jt}^W}) \tag{29}$$

$$0 \leq P_{t,s}^{spill} \leq \sigma_t / n \tag{30}$$

where (26) and (29) describe the possible load shedding and wind spillage that might occur during real-time operation, respectively. Equations (27) and (30) indicate that the amount of load shedding and wind spillage at each interval are limited to the width of their associated intervals, respectively.

3) Conventional unit constraint: In order to make the proposed AIO model more consistent with practical limitations, two types of reserve, power-capacity reserve and ramp-capability reserve, are modeled associated with each conventional generating unit. Power-capacity reserve ensures that sufficient online generation capacity is available when the wind power generation deviates from the predicted value. Ramp-capability reserve is required to cope with rapid fluctuations during any given period and large period-to-period variations in wind power. Accordingly, traditional period-to-period ramping constraints (8),(9) and short-term reserve constraints (10),(11) may not provide sufficient fast ramping ability in response to variation and uncertainty of the wind generation. Thus, upper and lower envelops for unit operation under AIs are determined by scheduling the power output and power-capacity reserve as illustrated in Fig. 2. Equations (31)-(34) are sets of constraints ensuring that a unit can provide any power trajectory within its upper and lower envelops. Constraints (31) and (32) represent short-term ramp-capability reserve. These constraints ensure that a generator is able to change its output from upper (lower) envelope to lower (upper) envelope in a short-term period ($A \leftrightarrow B$ in Fig. 2). The period-to-period ramp-capability constraints are presented in (33) and (34) which ensure that any period-to-period power trajectory within upper and lower envelops are restricted by the ramping up and down limits. In other words, constraints (33) and (34) respectively enforce the feasibility of maximum upwards and downwards power change that is possible within power-capacity operating range for adjacent operating hours ($B \rightarrow C$ and $A \rightarrow D$ in Fig. 2). Therefore, in addition to price offers for power-capacity reserve, units' ramping capability also affects the amount of reserve allocated to each unit.

$$0 \leq r_{it}^{dn} + r_{it}^{up} \leq v_{it} \overline{r_i^{up}} \tag{31}$$

$$0 \leq r_{it}^{up} + r_{it}^{dn} \leq v_{it} \overline{r_i^{dn}} \tag{32}$$

$$\begin{cases} P_{it}^G + r_{it}^{up} - P_{i,t-1}^G + r_{i,t-1}^{dn} \leq \\ \qquad RU_i v_{i,t-1} + SU_i (v_{it} - v_{i,t-1}) + \hat{M} (1 - v_{it}) \\ \hat{M} = \max(0, SU_i - RU_i - \underline{P_i^G}) \end{cases} \tag{33}$$

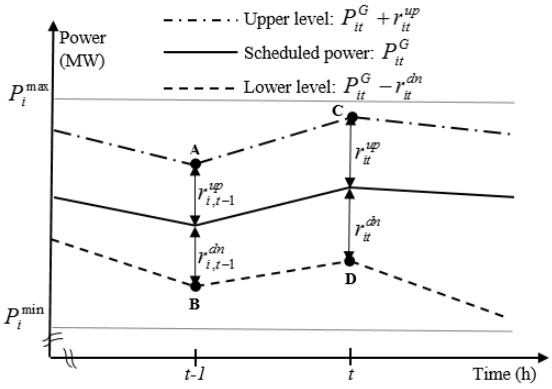

Fig. 2. Conventional unit's operating interval capability.

$$\begin{cases} P_{i,t-1}^G + r_{i,t-1}^{up} - P_{it}^G + r_{it}^{dn} \leq \\ \qquad RD_i v_{it} + SD_i (v_{i,t-1} - v_{it}) + \hat{N} (1 - v_{i,t-1}) \\ \hat{N} = \max(0, SD_i - RD_i - \underline{P_i^G}) \end{cases} \tag{34}$$

Finally, the proposed AIO model can be represented as

$$\begin{aligned} \min z = & \sum_{t=1}^{N_T} \sum_{i=1}^{N_G} (u_{it} C_{it}^{SU} + w_{it} C_{it}^{SD} + v_{it} C_{it}^F + C_{it}^V P_{it}^G \\ & + q_{it}^{up} r_{it}^{up} + q_{it}^{dn} r_{it}^{dn}) + \sum_{t=1}^{N_T} (C_t^{EENS} EENS_t + C_t^{EWS} EWS_t) \end{aligned} \tag{35}$$

s.t. (2)-(7),(20),(23)-(34)

$$\sum_{i=1}^{N_G} P_{it}^G + \sum_{i=1}^{N_G} r_{it}^{up} + \sum_{j=1}^{N_J} \underline{\hat{P}_{jt}^W} = \sum_{b=1}^{N_B} D_{bt} \tag{36}$$

$$\sum_{i=1}^{N_G} P_{it}^G - \sum_{i=1}^{N_G} r_{it}^{dn} + \sum_{j=1}^{N_J} \overline{\hat{P}_{jt}^W} = \sum_{b=1}^{N_B} D_{bt} \tag{37}$$

$$\begin{cases} -\sum_{j=1}^{N_J} \xi_{ljt} + \sum_{i=1}^{N_G} K_{li} \hat{P}_{it}^G + \sum_{j=1}^{N_J} K_{lj} \overline{\hat{P}_{jt}^W} - \sum_{b=1}^{N_B} K_{lb} D_{bt} \leq \overline{F_l} \\ \qquad \xi_{ljt} \geq 0, -\xi_{ljt} \leq K_{lj} \left(\underline{\hat{P}_{jt}^W} - \overline{\hat{P}_{jt}^W} \right) \end{cases} \forall l \in \Gamma \tag{38}$$

$$\begin{cases} \sum_{j=1}^{N_J} \vartheta_{ljt} + \sum_{i=1}^{N_G} K_{li} \hat{P}_{it}^G + \sum_{j=1}^{N_J} K_{lj} \overline{\hat{P}_{jt}^W} - \sum_{b=1}^{N_B} K_{lb} D_{bt} \geq -\overline{F_l} \\ \qquad \vartheta_{ljt} \geq 0, \vartheta_{ljt} \geq K_{lj} \left(\underline{\hat{P}_{jt}^W} - \overline{\hat{P}_{jt}^W} \right) \end{cases} \forall l \in \Gamma \tag{39}$$

$$-r_{it}^{dn} \leq \hat{P}_{it}^G - P_{it}^G \leq r_{it}^{up} \tag{40}$$

III. Case Studies

In order to examine the effectiveness of the proposed AIO model, an 8-bus and the modified IEEE 118-bus test systems are examined in this section. The proposed AIO model is an MILP problem that was solved using CPLEX 12.5.1 [27] under GAMS [28]. All optimization problems were solved on a 2.30-GHz Intel Core i5 CPU personal computer with 4GB of RAM memory. The gap tolerance for solving MIP was 0.05%.

A. 8-bus test system

The 8-bus test system includes 5 generators and 2 wind farms, as shown in Fig. 3. Generating unit characteristics and transmission lines information are given in the appendix. The generation capacity of wind farms WF1 and WF2 are 55 MW and 45 MW, respectively. System daily load curve and the

This article has been accepted for publication in a future issue of this journal, but has not been fully edited. Content may change prior to final publication. Citation information: DOI 10.1109/TSG.2016.2572639, IEEE Transactions on Smart Grid

forecasted production of wind farms are shown in Fig. 4. Daily peak load is 315 MW and it happens at hour 20. Since the forecast errors increase along with the time, errors ranging from 20% to 45% have been chosen for the wind farm PIs. The confidence level is set as 95% (i.e. $\gamma = 2$). The costs of energy not supplied and wind energy spilled are assumed to be 2500 \$/MWh and 100 \$/MWh, respectively.

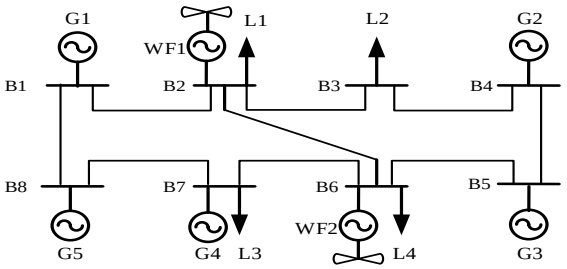

Fig. 3. 8-bus test system.

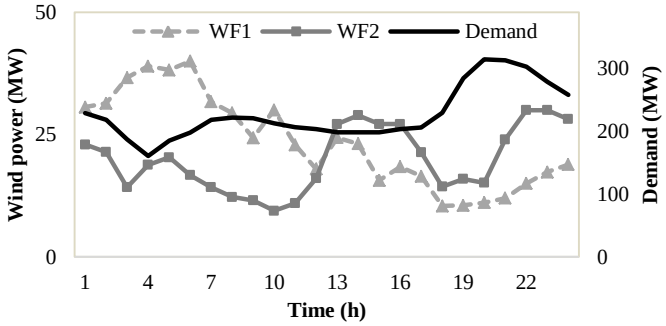

Fig. 4. System daily load curve and wind power forecast.

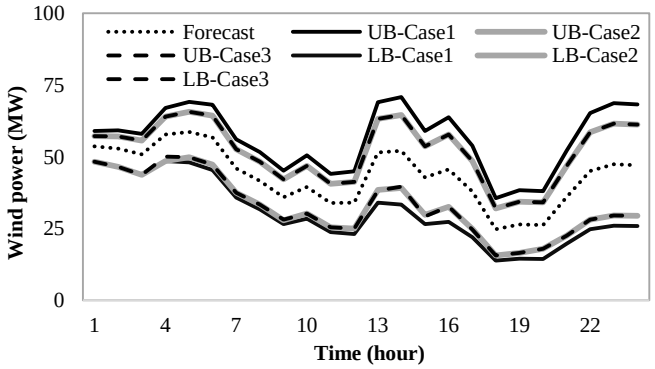

Fig. 5. Wind power uncertainty intervals.

1) Results and Verification: To demonstrate performance of the proposed AIO model, the following three cases are derived and discussed in details:

Case 1) The IO model described in Section II.A.

Case 2) The AIO model excluding ramp-capability reserve.

Case 3) The AIO model including ramp-capability reserve.

These cases are tackled using the formulation proposed previously and the solutions are presented in the following.

The total wind power generation and its associated uncertainty intervals are shown in Fig. 5, where UB and LB are upper and lower bounds of uncertainty intervals, respectively. It can be observed that utilizing the AIO model either excluding or including ramp-capability reserves results in rather narrower wind power uncertainty intervals. The reason is that the scenarios with low probabilities are not going to be covered by the reserve capacities. The other observation is that the awarded power-capacity reserve values associated with cases 2 and 3 are approximately the same while their ramping attribute substantially differ. This issue would be discussed in the following paragraph. Table I outlines the hourly commitment of generating units. As it is shown, units G1 and G2 are serving as the base units in all three cases. However, the narrower intervals for wind power uncertainty coverage would change the commitment status of units G3, G4, and G5 as highlighted in Table I. In case 2, the unit G5 which is more expensive than the other units is committed just at hours 8 and 9 to compensate the wind uncertainty intervals. The reason for this observation relies on unit G5 short minimum up-time along with small start-up and shut down costs. In addition, units G3 and G4 are committed an hour earlier compared to case 1. In case 3, with taking the ramp-capability reserve constraints into account, unit G4 is committed for the entire horizon due to its high ramp capability while the more expensive unit G5 is kept OFF.

TABLE I. COMMITMENT STATUS UNDER DIFFERENT CASES

Hour	G1			G2			G3			G4			G5		
	Case no.			Case no.			Case no.			Case no.			Case no.		
	1	2	3	1	2	3	1	2	3	1	2	3	1	2	3
1	1	1	1	1	1	1	0	0	0	0	0	1	0	0	0
2	1	1	1	1	1	1	0	0	0	0	0	1	0	0	0
3	1	1	1	1	1	1	0	0	0	0	0	1	0	0	0
4	1	1	1	1	1	1	0	0	0	0	0	1	0	0	0
5	1	1	1	1	1	1	0	0	0	0	0	1	0	0	0
6	1	1	1	1	1	1	0	0	0	0	0	1	0	0	0
7	1	1	1	1	1	1	0	0	0	0	0	1	0	0	0
8	1	1	1	1	1	1	0	0	0	0	0	1	1	1	0
9	1	1	1	1	1	1	0	0	0	0	0	1	1	1	0
10	1	1	1	1	1	1	0	0	0	0	0	1	1	0	0
11	1	1	1	1	1	1	0	0	0	0	0	1	1	0	0
12	1	1	1	1	1	1	0	0	0	0	0	1	1	0	0
13	1	1	1	1	1	1	0	0	0	0	0	1	1	0	0
14	1	1	1	1	1	1	0	0	0	0	0	1	1	0	0
15	1	1	1	1	1	1	0	0	0	0	0	1	1	0	0
16	1	1	1	1	1	1	0	0	0	0	0	1	1	0	0
17	1	1	1	1	1	1	0	0	0	0	0	1	1	0	0
18	1	1	1	1	1	1	0	0	0	0	1	1	1	0	0
19	1	1	1	1	1	1	0	1	1	1	1	1	1	0	0
20	1	1	1	1	1	1	1	1	1	1	1	1	1	0	0
21	1	1	1	1	1	1	1	1	1	1	1	1	0	0	0
22	1	1	1	1	1	1	1	1	1	1	1	1	0	0	0
23	1	1	1	1	1	1	1	1	1	1	1	1	0	0	0
24	1	1	1	1	1	1	1	1	1	1	1	1	0	0	0

Table II compares the market clearing results, including total generation, total upward and downward reserves, and their associated costs. It can be seen that the required upward (downward) reserve are reduced by 17.5% (33.5%) and 17.8% (33.5%) for cases 2 and 3, respectively. Consequently, the reserve cost is reduced by 29.8% and 25.4%, respectively. In addition, the fixed cost and generation cost are reduced as well. Although the difference of total upward and downward reserves between cases 2 and 3 is only about 1 MW, the difference in total reserve cost is about \$114 which is due to procuring more reserve from expensive but high ramp unit G4.

In order to verify the results obtained from the proposed AIO model, a comparison based on Monte Carlo simulation (MCS) is utilized. To do so, associated with all scenarios generated by MCS, a 10-min economic dispatch problem is solved. Then, the solution for envisaged cases are compared in terms of EENS, EWS, expected dispatch cost (EDC), and standard deviation (SD) of dispatch cost. The EDC and SD are

This article has been accepted for publication in a future issue of this journal, but has not been fully edited. Content may change prior to final publication. Citation information: DOI 10.1109/TSG.2016.2572639, IEEE Transactions on Smart Grid

the mean and standard deviation values of cumulative probability distribution function of dispatch cost obtained through the MCS approach. The results are outlined in the last three rows of Table II. In case 2 where the ramp-capability reserve is neglected, EWS and EENS increase to 3.864 MWh and 0.1728 MWh, respectively. Also, the EDC which indicates the economic efficiency of the solution increases by $895. The SD which represents the reliability of the real-time dispatch operation under the model decision rather deteriorates (102%). Referring to Table II, it is deduced that although the operation cost (sum of generation, reserve, and fixed costs at the day-ahead stage) slightly heightens in case 3 compared to case 2, the solution is much more reliable. As can be seen, EENS and EWS are reduced to 0.0096 MWh and 1.512 MWh, respectively. The EDC and its associated SD are improved as well. Therefore, having applied the proposed AIO model including ramp-capability reserve not only results in adjustable uncertainty intervals, but even can improve the efficiency and robustness of the system operation.

TABLE II. COMPARISON OF DIFFERENT CASES

Comparison Indices	Case 1	Case 2	Case 3
Total generation (MWh)	4410	4410	4410
Total upward/downward reserve (MW)	311.5/311.5	257/207	256/207
Total reserve cost ($)	2557	1793	1907
Total fixed cost* ($)	38100	34600	37200
Total generation cost ($)	146888	146191	146410
EWS/EENS (MWh)	1.8/ 0.0192	5.664/ 0.192	0.288/ 0.0096
Expected dispatch cost (EDC)($)	141800	142695	141592
Standard deviation (SD) ($)	1260	2553	1056

*Includes start-up, shut down, and fixed running costs

2) Sensitivity analysis on the confidence level: Setting an appropriate value for the confidence level is a crucial requirement for the system planners and operators letting them integrate wind power hedging higher operating costs or intensified operation risk. Evidently, the threshold value strongly depends on the system overall policies and regulations in procurement of reliable electricity service and it could be specified through different analytic or trial-and-error techniques. In order to scrutinize performance of the proposed model under different confidence levels, four case studies are examined and the results are presented in Table III. It can be seen that when the confident level is increased, the reliability of system operation will improve at the expense of higher operating cost and system reserve requirement. Accordingly, the confidence level is introduced in the proposed model to adjust the robustness and conservatism of the final solution. When the confidence level constraints, (22)-(23), is relaxed, its appropriate value with no limits is determined through the optimization procedure.

TABLE III. SENSITIVITY ANALYSIS ON CONFIDENCE LEVEL

Confidence level (%)	90	95	99	No limit
Total upward/ downward reserve (MW)	220/ 126	256/ 207	311.5/ 311.5	249/ 97
Operation cost ($)	178381	185517	195808	178432
EWS/ EENS (MWh)	5.976/ 0.840	0.288/ 0.0096	0.072/ 0.000	5.976/ 0.840
EDC ($)	144990	141592	141811	144990
SD ($)	5103	1056	1021	5103

Interestingly, two cases of 90% confidence level and relaxed confidence level have various reserve quantities but the same risk indices. This is due to identical generation scheduling of the units in two cases, which means that similar controllable resources are available to cope with variation and uncertainty of wind power during real-time operation. This observation reveals that reserve capacities are of dissimilar qualities and procurement costs.

3) Sensitivity analysis on the penalty costs: We change the values of the penalty costs for both load shedding and wind spillage from 100$/MWh to 6000$/MWh. The confidence level is assumed to be 95%. The results of upward and downward reserve schedules are depicted in Fig. 6.

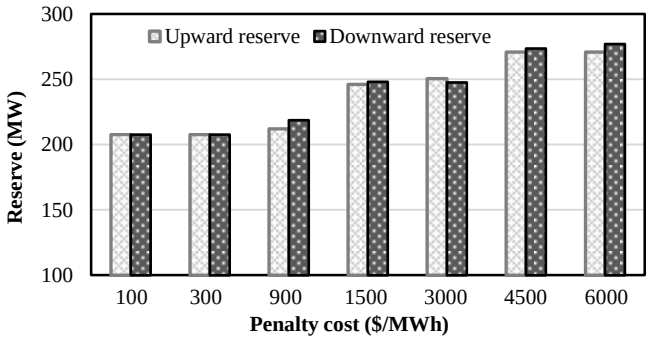

Fig. 6. Upward and downward reserve schedules under different penalty costs.

For small values of penalty costs, the scheduled reserves are almost constant due to confidence level limitation which does not allow that the system security is overly threatened by the optimality aspect of system operation. When the penalty costs are further on the rise, both up and down reserve capacities increase. In these circumstances, the confidence level does not constrain the solution and the problem optimality is the key factor in specifying the reserve quantities. For large values of the penalty costs, the scheduled reserves would not remarkably change. This saturation behavior is justified since in these situations the remaining tails of random distributions with very trivial probabilities do not have a significant effect in the objective function. In real practices, C_t^{EENS} and C_t^{EWS} can be selected as the value of loss load and expected social welfare loss of wind power spilled, respectively.

B. The Modified IEEE 118-bus Test System

The modified IEEE 118-bus test system has 54 generating units, 186 transmission lines, and 91 loads which is based on the one given in [29]. The original data is modified to include four wind farms at buses 22, 46, 68, and 86 with generation capacities of 315 MW, 390 MW, 390 MW, and 465 MW, respectively. The wind forecasts on a typical day (April 22, 2015) are used from the wholesale electricity market data of Ontario, Canada [30]. The wind forecast errors, confidence level, costs of EENS and EWS are the same as previous case study.

For the sake of comparison, the SO and RO methods are examined as well in addition to the proposed AIO model. The stochastic model is based on [5] which is a two-stage stochastic optimization problem. To this end, the MCS with Latin hypercube sampling technique [31] is utilized to generate 10000 scenarios representing plausible realizations of the stochastic process. Then, the number of generated scenarios is

This article has been accepted for publication in a future issue of this journal, but has not been fully edited. Content may change prior to final publication. Citation information: DOI 10.1109/TSG.2016.2572639, IEEE Transactions on Smart Grid

reduced to 20 scenarios via K-means clustering algorithm [32]. The robust model is based on [33], while the probable contingencies are ignored and the wind uncertainty is considered instead. For this purpose, PIs are employed to cover wind power uncertainty. We utilize a budget of uncertainty as suggested by [14] to adjust the conservatism of the model. In order to guarantee a robust optimal solution with probability approximately greater than 95%, the budget of uncertainty is set as 8 in this study [14].

In order to compare the above methods, the day-ahead schedules achieved by each model are tested using MCS (under 1000 scenarios) against various realizations of wind uncertainty. Table IV compares the economic performance, system security, and computation efficiency of three models. The economic performance consists of operation cost, reserve cost, EDC, and SD. As it can be seen, the AIO model operation cost is slightly higher than SO (0.3% increment), and is 0.6% less than the one obtained by RO. However, SD of EDC associated with the AIO model is the lowest indicating the reliability and low variation of real-time dispatch.

In Table IV, the insecure scenarios are the scenarios where the given schedule results fail to meet the system security constraints for at least one operating hour. The outcomes are also quantified by the frequency of load shedding and wind spillage occurrence denoted by freq. The security level is the ratio of secure scenarios to all scenarios. Referring to Table IV, it is clear that due to ramping capability of the procured reserve in the AIO model, there exists only one unsecure scenario and the system security level is highly guaranteed.

Additionally, the AIO model is the most efficient method in terms of computational time. Compared to standard two-stage RO and SO, the computational time of the AIO model is reduced by 47.1% and 96.9%, respectively, which is a very desirable feature for real-world practices.

TABLE IV. COMPARISON OF SO, RO, AND PROPOSED AIO MODELS

Comparison Indices	AIO model	SO	RO
Operation cost ($)	1182338 (99.4%)	1177810 (99.1%)	1188408 (100%)
Total reserve cost ($)	15656(82%)	11204(59%)	18984(100%)
EWS/ EENS (MWh)	0/0.024	0/3.072	0/0.192
EDC ($)	1163356	1164281	1167748
SD ($)	4966	32927	6473
Number of insecure scenarios (freq.)	1 (1)	143 (220)	11 (23)
Security level (%)	99.9	85.7	98.9
CPU time (Second)	35 (3.1%)	1130(100%)	563(50.2)

IV. CONCLUSION

In this paper, a novel model was proposed for day-ahead energy and reserve market clearing to improve the system security against variation and uncertainty of wind power. The model calculates AIs for wind farms to cope with wind uncertainty in an economic way. Ramp-capability reserve was also modeled to provide enough ramp ability to follow the expected maximum variation within the AIs. AIs can be controlled by varying the confidence level to adjust the conservatism of the solution. The simulation results demonstrated that by applying the proposed AIO, the PIs can be adjusted to economically cover wind uncertainty while ensuring a robust solution. Sensitivity analysis showed that choosing an appropriate value for confidence level in the AIO could improve the system ability to absorb more wind power while averting high operating costs. Compared with SO and RO, the AIO model is much more secure while its costs is slightly higher than SO. Besides, since the AIO addresses the uncertainty of wind power in a compact way, it is very efficient in terms of computation performance and it can be adopted in large-scale power systems.

APPENDIX

A. Data of 8-Bus System

Table AI lists the generator data for 8-bus system. Table AII lists transmission line data for 8-bus system.

TABLE AI. GENERATOR DATA FOR 8-BUS TEST SYSTEM

Unit	G1	G2	G3	G4	G5
C_{it}^{SU}	2550	2250	2100	2000	1500
C_{it}^{SD}	1200	1100	1050	1000	750
C_{it}^{F}	500	400	450	450	400
C_{it}^{V}	32	34	36	36	38
q_{it}^{up}, q_{it}^{dn}	3	4	5	5	6
$\overline{P_i^G}$	100	90	75	72	50
$\underline{P_i^G}$	25	15	10	10	10
$\overline{r_i^{up}}, \overline{r_i^{dn}}$	5	8	10	12	10
SU_i, SD_i	30	40	50	55	50
RU_i, RD_i	30	40	50	55	50
UT_i, DT_i	5	4	3	3	2

TABLE AII. TRANSMISSION LINE DATA FOR 8-BUS TEST SYSTEM

From bus	To bus	X(p.u.)	Transmission Limit (MW)
1	2	0.12	80
1	8	0.38	50
2	3	0.24	60
2	6	0.08	80
3	4	0.40	44
4	5	0.08	80
5	6	0.17	80
6	7	0.16	70
7	8	0.08	80

B. Interval Wind Power Optimization Model

In the market clearing model presented in Section II.A, constraints (12) and (13) should be satisfied for all possible uncertain parameters within the PIs. At first, let represent $\tilde{P}_{jt}^{w}$ in the following way by introducing a new continuous variable β_{jt} which has the value between 0 and 1.

$$\tilde{P}_{jt}^{w} = \beta_{jt} \underline{P_{jt}^{W}} + \left(1-\beta_{jt}\right)\overline{P_{jt}^{W}} \quad \text{(A1)}$$

Therefore, (12) and (13) can be presented as in (A2) and (A3), respectively.

$$\sum_{i=1}^{N_G} P_{it}^{G} + \sum_{i=1}^{N_G} r_{it}^{up} + \sum_{j=1}^{N_J}\left(\beta_{jt}\underline{P_{jt}^{W}} + \left(1-\beta_{jt}\right)\overline{P_{jt}^{W}}\right) = \sum_{b=1}^{N_B} D_{bt}, \forall \beta_{jt} \in [0,1] \quad \text{(A2)}$$

This article has been accepted for publication in a future issue of this journal, but has not been fully edited. Content may change prior to final publication. Citation information: DOI 10.1109/TSG.2016.2572639, IEEE Transactions on Smart Grid

$$-\overline{F_l} \le \sum_{b=1}^{N_B} K_{lb} \left(\begin{array}{l} \sum_{i \in I_b} \tilde{P}_{it}^G + \sum_{j \in J_b} \beta_{jt} \underline{P_{jt}^W} + \\ \sum_{j \in J_b} \left(1-\beta_{jt}\right) \overline{P_{jt}^W} - D_{bt} \end{array} \right) \le \overline{F_l}, \forall l \in \Gamma, \forall \beta_{jt} \in [0,1] \quad \text{(A3)}$$

These constraints will be violated, if reserve in both upward and downward directions under network constraints are not sufficiently provided. Accordingly, we should guarantee the system security by satisfying the following four worst-case scenarios:

1) The worst-case scenario for the upward reserve constraint is

$$\begin{cases} \delta_t^u = \min\limits_{\beta_{jt}^1} \left(\sum\limits_{i=1}^{N_G} \left(P_{it}^G + r_{it}^{up}\right) + \sum\limits_{j=1}^{N_J} \left(\beta_{jt}^1 \underline{P_{jt}^W} + \left(1-\beta_{jt}^1\right) \overline{P_{jt}^W} \right) - \sum\limits_{b=1}^{N_B} D_{bt} \right) \ge 0 \\ s.t. \qquad 0 \le \beta_{jt}^1 \le 1 \end{cases} \quad \text{(A4)}$$

where δ_t^u is the minimum value of the upward reserve for the system when the wind uncertainty is revealed, and it must be greater than or equal to zero to avoid potential load shedding. Substituting (12) by (A4), the market clearing model becomes a two-layer optimization problem which cannot be solved effectively. Applying the duality theory, the model can be transformed into a single-level robust counterpart [19]. The corresponding dual problem of (A4) is

$$\begin{cases} \max\limits_{\varphi_{jt}} \left(\sum\limits_{i=1}^{N_G} P_{it}^G + \sum\limits_{i=1}^{N_G} r_{it}^{up} + \sum\limits_{j=1}^{N_J} \overline{P_{jt}^W} - \sum\limits_{j=1}^{N_J} \varphi_{jt} - \sum\limits_{b=1}^{N_B} D_{bt} \right) \\ s.t. \qquad -\varphi_{jt} \le \left(\underline{P_{jt}^W} - \overline{P_{jt}^W} \right), \varphi_{jt} \ge 0 \end{cases} \quad \text{(A5)}$$

where φ_{jt} is the dual variable of (A2). From the duality theory, the following formula holds

$$\sum_{j=1}^{N_J} \beta_{jt}^1 \underline{P_{jt}^W} + \left(1-\beta_{jt}^1\right) \overline{P_{jt}^W} \le \sum_{j=1}^{N_J} \overline{P_{jt}^W} - \sum_{j=1}^{N_J} \varphi_{jt} \quad \text{(A6)}$$

Therefore, (A2) is equivalent to (A7) for this scenario and it can be presented as in (15).

$$\begin{cases} \left(\sum\limits_{i=1}^{N_G} P_{it}^G + \sum\limits_{i=1}^{N_G} r_{it}^{up} + \sum\limits_{j=1}^{N_J} \overline{P_{jt}^W} - \sum\limits_{j=1}^{N_J} \varphi_{jt} \right) \ge \sum\limits_{b=1}^{N_B} D_{bt} \\ -\varphi_{jt} \le \left(\underline{P_{jt}^W} - \overline{P_{jt}^W} \right), \varphi_{jt} \ge 0 \end{cases} \quad \text{(A7)}$$

2) The worst-case scenario for the downward reserve constraint is

$$\begin{cases} \delta_t^d = \min\limits_{\beta_{jt}^2} \left(\sum\limits_{b=1}^{N_B} D_{bt} - \sum\limits_{i=1}^{N_G} \left(P_{it}^G - r_{it}^{dn}\right) - \sum\limits_{j=1}^{N_J} \left(\beta_{jt}^2 \underline{P_{jt}^W} + \left(1-\beta_{jt}^2\right) \overline{P_{jt}^W} \right) \right) \ge 0 \\ s.t. \qquad 0 \le \beta_{jt}^2 \le 1 \end{cases} \quad \text{(A8)}$$

where δ_t^d is the minimum value of the system-wide downward reserve for all realization of wind power within the PIs, and it should be greater than or equal to zero to prevent potential wind spillage. Similar to the upward reserve, constraint (A2) can be expressed as in (A9) for this scenario, where ψ_{jt} is the dual variable of (A8). Finally, (A9) can be presented as in (16).

$$\begin{cases} \left(\sum\limits_{i=1}^{N_G} P_{it}^G - \sum\limits_{i=1}^{N_G} r_{it}^{dn} + \sum\limits_{j=1}^{N_J} \overline{P_{jt}^W} + \sum\limits_{j=1}^{N_J} \psi_{jt} \right) \le \sum\limits_{b=1}^{N_B} D_{bt} \\ \psi_{jt} \ge \left(\underline{P_{jt}^W} - \overline{P_{jt}^W} \right), \psi_{jt} \ge 0 \end{cases} \quad \text{(A9)}$$

3) The worst-case scenario for the positive line flow constraint is

$$LF_{lt}^u = \max_{\beta_{jt}^3} \left(\begin{array}{l} \sum_{i=1}^{N_G} K_{li} \tilde{P}_{it}^G - \sum_{b=1}^{N_B} K_{lb} D_{bt} + \\ \sum_{j=1}^{N_J} K_{lj} \left(\beta_{jt}^3 \underline{P_{jt}^W} + \left(1-\beta_{jt}^3\right) \overline{P_{jt}^W} \right) \end{array} \right) \le \overline{F_l} \quad \text{(A10)}$$

where LF_{lt}^u represents the maximum positive line flow under the network worst-case scenario, and it should lie within its upper limit to ensure the network security.

4) The worst-case scenario for the negative line flow constraint is

$$LF_{lt}^d = \min_{\beta_{jt}^4} \left(\begin{array}{l} \sum_{i=1}^{N_G} K_{li} \tilde{P}_{it}^G - \sum_{b=1}^{N_B} K_{lb} D_{bt} + \\ \sum_{j=1}^{N_J} K_{lj} \left(\beta_{jt}^4 \underline{P_{jt}^W} + \left(1-\beta_{jt}^4\right) \overline{P_{jt}^W} \right) \end{array} \right) \ge -\overline{F_l} \quad \text{(A11)}$$

where LF_{lt}^d is the minimum negative line flow under the network worst-case scenario, and it should lie within its lower limit for the operational security of the network. With the idea introduced for the upward reserve constraint, (A10) and (A11) can be presented as in (17) and (18).

REFERENCES

[1] H. Nosair and F. Bouffard, "Flexibility envelopes for power system operational planning," *IEEE Trans. Sustain. Energy*, vol. 6, no. 3, pp. 800–809, 2015.

[2] L. Xu, "Flexible Ramping Products," CAISO Market Development and Analysis, Draft Final Proposa, April 2012. [Online]. Available: http://www.caiso.com/Documents/DraftFinalProposal-FlexibleRampingProduct.pdf.

[3] N. Navid and G. Rosenwald, "Ramp capability product design for MISO markets," MISO Market Development and Analysis, July 2013. [Online]. Available: https://www.misoenergy.org/_layouts/miso/ecm/redirect.aspx?id=156879.

[4] F. Bouffard and F. D. Galiana, "Stochastic security for operations planning with significant wind power generation," *IEEE Trans. Power Syst.*, vol. 23, no. 2, pp. 306-316, 2008.

[5] J. M. Morales, A. J. Conejo, and J. Perez-Ruiz, "Economic valuation of reserves in power systems with high penetration of wind power," *IEEE Trans. Power Syst.*, vol. 24, no. 2, pp. 900-910, 2009.

[6] A. Papavasiliou, S. S. Oren, and R. P. O'Neill, "Reserve requirements for wind power integration: A scenario-based stochastic programming framework," *IEEE Trans. Power Syst*, vol. 26, no. 4, pp. 2197-2206, 2011.

[7] A. Papavasiliou, S. S. Oren, and B. Rountree, "Applying high performance Computing to Transmission-Constrained Stochastic Unit Commitment for Renewable Energy Integration," *IEEE Trans. Power. Syst.*, vol. 30, no. 3, pp. 1109-1120, 2015.

[8] J. M. Morales, S. Pineda, A. J. Conejo, and M. Carrion, "Scenario reduction for futures market trading in electricity markets," *IEEE Trans. Power Syst.*, vol. 24, no. 2, p. 878–888, 2009.

[9] M. Kaut and S. W. Wallace, "Evaluation of scenario-generation methods for stochastic programming," *Stochastic Program.*, vol. 3, no. 2, p. 257–271, 2007.

[10] L. Wu, M. Shahidehpour, and Z. Li, "Comparison of scenario-based and

interval optimization approaches to stochastic SCUC," *IEEE Trans. Power Syst.*, vol. 27, no. 2, p. 913–921, 2012.

[11] U. A. Ozturk, M. Mazumdar, and B. A. Norman, "A solution to the stochastic unit commitment problem using chance constrained programming," *IEEE Trans. Power Syst.*, vol. 19, no. 3, pp. 1589-1598, 2004.

[12] Q. Wang, Y. Guan, and J. Wang, "A chance-constrained two-stage stochastic program for unit commitment with uncertain wind power output," *IEEE Trans. Power Syst.*, vol. 27, no. 1, pp. 206-215, 2012.

[13] H. Wu, M. Shahidehpour, Z. Li, and W. Tian, "Chance-constrained day-ahead scheduling in stochastic power system operation," *IEEE Trans. Power Syst.*, vol. 29, no. 4, pp. 1583-1591, 2014.

[14] B. Hu and L. Wu, "Robust SCUC considering continuous/discrete uncert- ainties and quick-start units: a two-stage robust optimization with mixed-integer recourse," *IEEE Trans. Power Syst.*, vol. 31, no. 2, pp. 1407-1419, 2016.

[15] R. Jiang, J. Wang, and Y. Guan, "Robust unit commitment with wind power and pumped storage hydro," *IEEE Trans. Power Syst.*, vol. 27, no. 2, pp. 800-810, 2012.

[16] Y. Guan and J. Wang, "Uncertainty sets for robust unit commitment," *IEEE Trans. Power Syst.*, vol. 29, no. 3, pp. 1439-1440, 2014.

[17] W. Wei, F. Liu, S. Mei, and Y. Hou, "Robust Energy and Reserve Dispatch under Variable Renewable Generation," *IEEE Trans. Smart Grid*, vol.6, no.1, pp.369-380, 2015.

[18] C. Zhao and Y. Guan, "Unified Stochastic and Robust Unit Commitment," *IEEE Trans. Power Syst.*, vol. 28, no. 3, p. 3353–3361, 2013.

[19] D. Bertsimas and M. Sim, "The Price of Robustness," *Operations Research*, vol. 52, no. 1, pp. 35-53, 2004.

[20] A. Lorca and X. Sun, "Adaptive robust optimization with dynamic uncertainty sets for multi-period economic dispatch under significant wind," *IEEE Trans. Power Syst.*, vol. 30, no. 4, p. 1702–1713, 2015.

[21] Y. Wang, Q. Xia, and C. Kang, "Unit commitment with volatile node injections by using interval optimization," *IEEE Trans. Power Syst.*, vol. 26, no. 3, p. 1705–1713, 2011.

[22] Y. Yu, P. B. Luh, E. Litvinov, T. Zheng, J. Zhao, and F. Zhao, "Grid integration of distributed wind generation: hybrid markovian and interval unit commitment," *IEEE Trans. Smart Grid*, vol.6, no.6, pp.3061-3072, 2015.

[23] Y. Dvorkin, H. Pandžić, M. A. Ortega-Vazquez, and D. S. Kirschen, "A hybrid stochastic/interval approach to transmission-constrained unit commitment," *IEEE Trans. Power Syst.*, vol. 30, no. 2, p. 621–631, 2015.

[24] R. Madani, J. Lavaei, and R. Baldick, "Constraint screening for security analysis of power networks," Preprint 2015, [Online]. Available: http://www.ieor.berkeley.edu/~lavaei/SC-Screening-2015.pdf.

[25] A. J. Ardakani and F. Bouffard, "Identification of Umbrella Constraints in DC-Based Security-Constrained Optimal Power Flow," *IEEE Trans. Power Syst.*, vol. 28, no. 4, p. 3924–3934, 2013.

[26] A. Papoulis and S. U. Pillai, Probability, random variables, and stochastic processes, Tata McGraw-Hill Education, 2002.

[27] The GAMS/CPLEX manual, [Online]. Available: http://www. gams. com/dd/docs/solvers/cplex/index.html.

[28] The General Algebraic Modeling System (GAMS) Software, [Online]. Available: http://www.gams.com.

[29] [Online]. Available: http://motor.ece.iit.edu/data/JEAS_IEEE118.

[30] Independent Electricity System Operator (IESO), Ontario, Canada, [Online]. Available: http://www.ieso.ca/.

[31] J. Wang, M. Shahidehpour, and Z. Li, "Security-constrained unit commitment with volatile wind power generation," *IEEE Trans. Power Syst.*, vol. 23, no. 3, p. 1319–1327, 2008.

[32] L. Baringo and A. J. Conejo, "Correlated wind-power production and electric load scenarios for investment decisions," *Applied Energy*, vol. 101, p. 475–482, 2013.

[33] A. Street, A. Moreira, and J. Arroyo, "Energy and reserve scheduling under a joint generation and transmission security criterion: An adjustable robust optimization approach," *IEEE Trans. Power Syst.*, vol. 29, no. 1, p. 3–14, 2014.